Reconstructing positive and negative couplings in Ising spin networks by sorted local transfer entropy

Felix Goetze and Pik-Yin Lai*

Department of Physics and Center for Complex Systems, National Central University, Chung-Li District, Taoyuan City 320, Taiwan, Republic of China

and Molecular Science and Technology Program, Taiwan International Graduate Program, Academia Sinica, Taipei, Taiwan, Republic of China

(Received 15 February 2019; published 16 July 2019)

We employ the sorted local transfer entropy (SLTE) to reconstruct the coupling strengths of Ising spin networks with positive and negative couplings (J_{ij}), using only the time-series data of the spins. The SLTE method is model-free in the sense that no knowledge of the underlying dynamics of the spin system is required and is applicable to a broad class of systems. Contrary to the inference of coupling from pairwise transfer entropy, our method can reliably distinguish spin pair interactions with positive and negative couplings. The method is tested for the inverse Ising problem for different J_{ij} distributions and various spin dynamics, including synchronous and asynchronous update Glauber dynamics and Kawasaki exchange dynamics. It is found that the pairwise SLTE is proportional to the pairwise coupling strength to a good extent for all cases studied. In addition, the reconstruction works well for both the equilibrium and nonequilibrium cases of the time-series data. Comparison to other inverse Ising problem approaches using mean-field equations is also discussed.

DOI: 10.1103/PhysRevE.100.012121

I. INTRODUCTION

Many systems of interest in physics, biology, and social science are multicomponent, with the different components interacting with each other. One of the ultimate goals in bridging experimental data and theoretical understanding in a multicomponent interacting complex system is trying to answer the following question: "Which entities are interacting with each other and what are the associated coupling strengths?" An accurate solution to such a question can also provide new insights and deep understanding on the fundamental mechanisms behind the complex phenomena. The answers to these questions can provide significant insights and understanding of the fundamental mechanism behind the overall behavior of the systems. Lots of experimental data have been measured for various complex networks of interest, particularly in physical, biological, atmospheric, and social sciences. Successful methods for uncovering knowledge from data should be very general and can be widely applicable to different areas, and thus are expected to give deep and broad impacts. It has been suggested [1] that the structure of a network controls its dynamics and thus information about the network structure can be uncovered from their dynamics. The problem of reconstructing networks from dynamics has become a grand challenge in the field of network science and has attracted much research interest (see, e.g., [2,3] for review).

Despite the vast amount of data, there remains a big challenge to utilize the experimental measurements to answer the above questions and to obtain theoretical understanding of the systems. There is so far no entirely satisfactory method for the inverse problem of uncovering the detail internode couplings together with their strengths, sign, and directions accurately. Ideally, one should aim for model-free methods, i.e., no prior knowledge about the details of node dynamics and coupling functional form is needed. For example, we do not need other extra information such as nodal dynamics or the responses of the systems upon perturbations as required in previous studies [4–8]. Only data of the system dynamics, passively recorded or observed, are sufficient for practical applications. Some successful reconstructions have been achieved based on the relation between the dynamical correlations of the time-series data and the structure of a network under noises [9–13].

In another aspect, there has been recently reviving interests on the traditional Ising model with pairwise coupling J_{ij} between spins i and j in the context of the "inverse Ising problem" [14–23], which aims at reconstructing the coupling strength matrix J_{ij} solely from the measurement of the time-series data of the spin dynamics. Most approaches on the inverse Ising problem employ mean-field theories and by computing the spin correlation functions [14–18,21] one can get rather satisfactory results if the underlying spin dynamics of the Ising model is known. On the other hand, reconstruction based on information theoretical quantities, such as mutual information or transfer entropy [24,25], are used less, although it is known that transfer entropy can reveal important information and signatures for the Ising model near phase transitions [26–30].

Transfer entropy (TE) [24,25] and its extensions have recently become more and more popular for the above task and have been applied to various types of neuronal data, such as from EEG, calcium imaging, and multi-electrode array measurements [31,32]. Being based on information theory, TE can be interpreted as the predictive information transfer

*pylai@phy.ncu.edu.tw

between two time series. TE is a model-free measurement and quantifies both linear and nonlinear interactions and their directionality. However, due to its information-theoretic nature, TE cannot distinguish between different types of interactions, for example, whether a presynaptic neuron drives a postsynaptic neuron via an excitatory or an inhibitory synapse [33]. This distinction is crucial for the understanding of the network dynamics and the exact interplay of excitation and inhibition in neuronal networks plays an important role for network bursts and synchronization [34–37]. High information transfer between two spike trains is expected for an underlying excitatory synapse between the neurons, but even inhibitory synapses show significant information transfer when observing sufficient spiking activity. In addition, TE has a thermodynamic meaning [38,39], and can be applied to extract useful information in social networks [40,41] and even linguistics studies [42].

In this work, we propose a method complementary to the TE measurement, which not only can measure the information transfer between the nodes, but also determine whether the coupling interactions are positive or negative. We achieve this by introducing a new quantity, which is a linear combination of the individual terms that sum up to the TE. To distinguish these type of interactions we analyze the local transfer entropies of each interaction and define the sorted local transfer entropy (SLTE) [43] that can faithfully reveal the sign and magnitude of the coupling interactions. The method does not depend on the detailed knowledge of the dynamics of the systems and is a technique to classify local TEs in such a way that can to spell out the underlying interactions accurately. Using various kinetic Ising models, we demonstrate that SLTE can achieve the goal of reconstructing the sign and relative coupling strengths in the inverse Ising problem for time-series data taken from equilibrium or nonequilibrium conditions without the knowledge of the underlying dynamical model.

II. TRANSFER ENTROPY AND SORTED LOCAL TRANSFER ENTROPY

Transfer entropy from a process Y to another process X is a measure that quantifies directional, nonlinear interactions between the two corresponding time-series x_n and y_n, which is the amount of uncertainty reduced in future values of X by knowing the past values of Y given past values of X. It is quantitatively defined as the difference of entropy rates (given by the conditional Shannon entropy) as

$$T_{Y\to X} = h_2 - h_1, \quad \text{where} \tag{1}$$

$$h_1 = -\sum_{x_{n+1},x_n,y_n} p(x_{n+1},x_n,y_n)\log_2 p(x_{n+1}|x_n,y_n), \tag{2}$$

$$h_2 = -\sum_{x_{n+1},x_n,y_n} p(x_{n+1},x_n,y_n)\log_2 p(x_{n+1}|x_n). \tag{3}$$

$T_{Y\to X}$ can be written as the Kullback entropy [24] as

$$T_{Y\to X} = \sum_{x_{n+1},x_n,y_n} p(x_{n+1},x_n,y_n)\log_2\left(\frac{p(x_{n+1}|x_n,y_n)}{p(x_{n+1}|x_n)}\right), \tag{4}$$

which can be interpreted as the information transfer from Y to X. The TE defined in Eq. (4) measures the information transfer that occurs at one time-step delay to model a first-order Markov process, but it can be generalized to higher orders by increasing the embedding lengths of the target and history processes [25]. The local TE from y to x is defined as [44] $\log_2\left(\frac{p(x_{n+1}|x_n,y_n)}{p(x_{n+1}|x_n)}\right)$ in Eq. (4).

There has been some research to infer the coupling strengths for Ising models by evaluating the TE for pairwise spins [45]. But due to the fact that TE is a nonnegative quantity regardless of the ferromagnetic or antiferromagnetic nature of the interactions, measurement of TE cannot reveal the sign of coupling between the spin pairs. Furthermore, as will be shown below, even when all couplings are positive, pairwise TE will increase with the coupling strength nonlinearly which renders the quantitative reconstruction of coupling strengths less practical for application.

To distinguish the sign of the interaction from Y to X, we note that although the TE given by Eq. (4) is always nonnegative, the local TE [44] in the sum can be positive or negative, meaning that y_n is "informative" or misinformative to x_{n+1}, respectively. The local TE in the sum in Eq. (4) is positive if $p(x_{n+1}|x_n,y_n) > p(x_{n+1}|x_n)$ or $p(x_{n+1},y_n|x_n) > p(y_n|x_n)p(x_{n+1}|x_n)$; i.e., the two states x_{n+1} and y_n occur together at a joint probability which is larger than the probability under assumed independence, signifying that the history y_n is informative to the future x_{n+1}. Similarly, if the history y_n is misinformative to the future x_{n+1}, the term would be negative. Thus to take into account of the nature of the interaction from y to x, one can properly weight or sort the local TE by its sign [43]. A similar concept of local or pointwise mutual information can help to extract useful information [46,47].

For the two-state Ising model, the time-series x_n and y_n take values of 1 or -1 for up and down spins, respectively. For the ferromagnetic and antiferromagnetic interactions between two spins the corresponding local transfer entropies reverse signs. In a ferromagnetic interaction, an up spin in a source node is informative about an up spin in a target node, while this would be misinformative for an antiferromagnetic interaction. Similarly, observing opposite valued spins in the source and target node is misinformative for a ferromagnetic interaction, but informative for an antiferromagnetic interaction. The strength of the ferromagnetic interaction is characterized not only by how informative aligned spins between the nodes are, but also by how misinformative the misaligned spins are, and vice versa for the antiferromagnetic interaction. By applying a positive multiplier to local transfer entropies from aligned spins and a negative multiplier to local transfer entropies from misaligned spins we have only positive contributions from the local transfer entropy terms for ferromagnetic interactions and only negative contributions from those terms for the antiferromagnetic interactions. Weighting these terms by the joint probabilities and summing over them, we get a quantity that is positive for ferromagnetic interactions and negative for antiferromagnetic interactions. Hence we define the sorted local transfer entropy (SLTE) as

$$T^{\text{sloc}}_{Y\to X} = \sum_{x_{n+1},x_n,y_n} x_{n+1}y_n p(x_{n+1},x_n,y_n)\log_2\left(\frac{p(x_{n+1}|x_n,y_n)}{p(x_{n+1}|x_n)}\right). \tag{5}$$

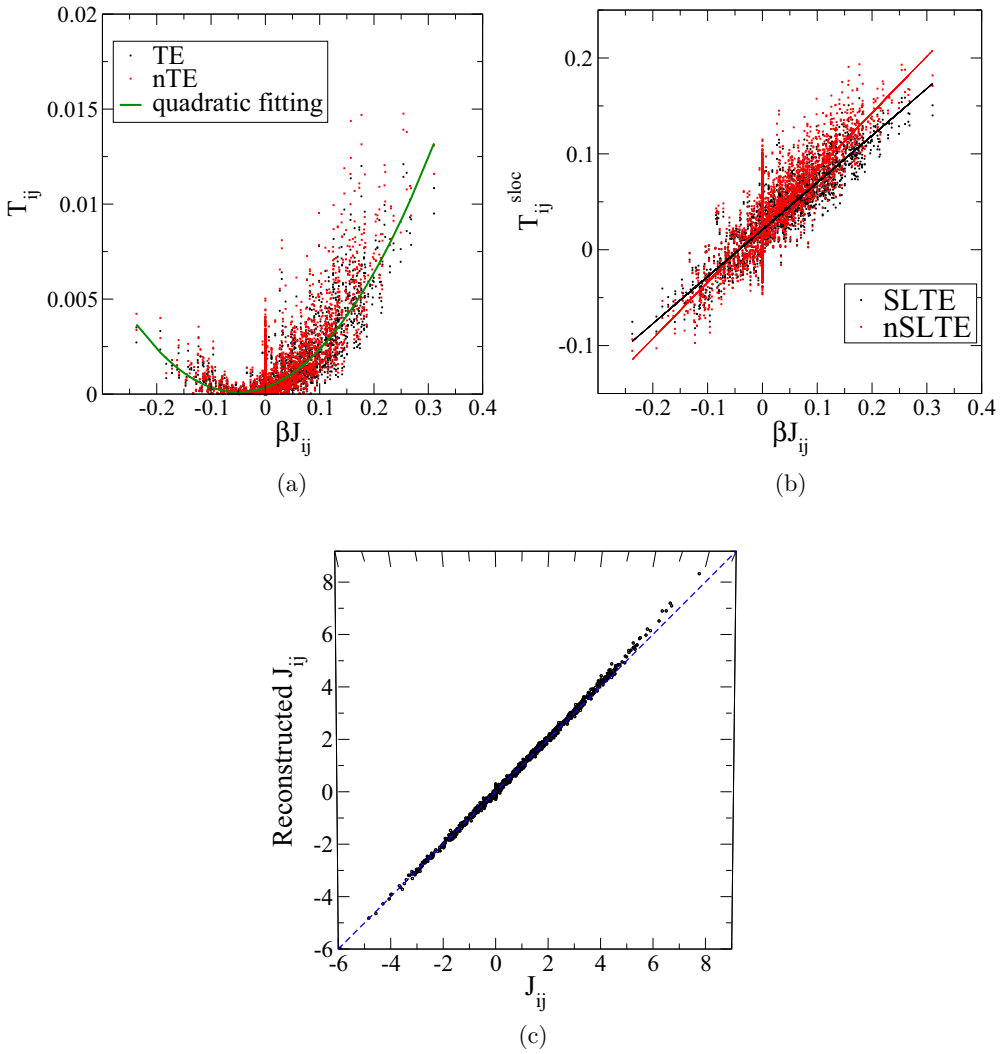

FIG. 1. Reconstruction of Ising spin couplings with Glauber spin dynamics on a bidirectional weighted random network using TE and SLTE. Dynamics are generated by a 10^5 MCS/spin transient period for equilibration and then time-series of length 10^5 is used for coupling reconstruction. (a) T_{ij} (TE) and normalized T(nTE) for every node pair ij vs. the actual coupling J_{ij}. A quadratic fitting for the TE (solid curve) is also shown. (b) $T^{\rm sloc}_{ij}$ (SLTE) and normalized $T^{\rm sloc}_{ij}$ (nSLTE) for every node pair ij vs. the actual coupling J_{ij}. The linear fits (solid lines) are also shown. The correlation coefficient between nSLTE and J $\simeq 0.75$. (c) Reconstructed J_{ij} vs. the actual ones using Eq. (8). The dashed line is $y = x$.

SLTE can be computed directly from the time-series data of y_n and x_n to deduce their pairwise interaction.

Since the magnitude of TE and SLTE would depend on the temporal variations of the time-series, it would make sense to normalize their values in some proper way. The entropy rate reflects the activity of the system to some extent, and the target entropy rate is the maximum possible transferred entropy, therefore the SLTE and TE are normalized by the target entropy rate to allow for a better comparison of situations of different activities. Here we define the normalized SLTE (nSLTE) from $Y \to X$ as the SLTE relative to the entropy rate of X [31,48]

$$\frac{T^{\rm sloc}_{Y\to X}}{-\sum_{x_{n+1},x_n} p(x_{n+1},x_n)\log_2 p(x_{n+1}|x_n)}. \tag{6}$$

TE can also be normalized (denoted by nTE) in a similar way.

III. ISING SPIN NETWORK RECONSTRUCTION USING SLTE

We consider Ising spin networks consisting of N spins, the dynamics of node i is given by the Ising spin s_i which can take value 1 or -1, and nodes can interact via pairwise interactions J_{ij} between spins i and j. In general, the matrix $\mathbf{J}$ can be asymmetric and can take positive or negative values. The conventional Ising model to describe equilibrium states is given by the Hamiltonian $\mathcal{H} = -\sum_{i,j} J_{ij}s_i s_j$, and follows the Boltzmann distribution $P(\vec{s}) \propto \exp[-\mathcal{H}/(k_B T)]$ at equilibrium with temperature T, where k_B is the Boltzmann constant. Each spin is a node on a network whose edges are indicated by nonzero values of J_{ij}. Random networks [49,50] of $N = 100$ and connection probability $p = 0.2$ are used in Monte Carlo simulations to test our results. Both directed and undirected(bidirectional) random networks are considered. The J_{ij} couplings for the bidirectional random networks

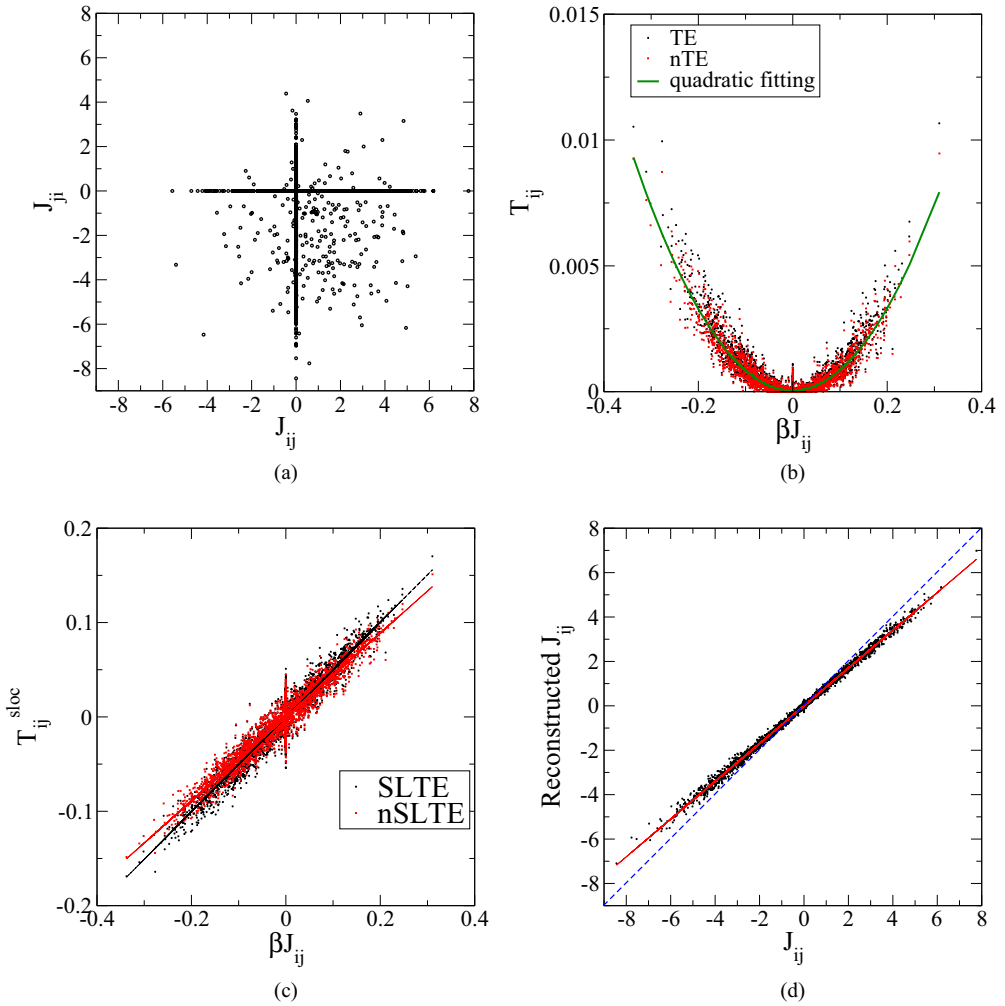

FIG. 2. Reconstruction of Ising spin couplings with asynchronous-update spin dynamics on a directed weighted random network using TE and SLTE. Dynamics are generated by a 10^5 MCS/spin transient period for equilibration and then time-series of length 10^5 is used for coupling reconstruction. (a) J_{ji} vs. J_{ij} showing the asymmetric couplings in the directed network. (b) T_{ij} (TE) and normalized T (nTE) for every node pair ij vs. the actual coupling J_{ij}. A quadratic fitting for the TE (solid curve) is also shown. (c) $T_{ij}^{\rm sloc}$ (SLTE) and normalized $T_{ij}^{\rm sloc}$ (nSLTE) for every node pair ij vs. the actual coupling J_{ij}. The linear fits (solid lines) are also shown. The correlation coefficient between nSLTE and $J \simeq 0.90$. (d) Reconstructed J_{ij} vs. the actual ones using Eq. (10). The dashed line is $y = x$.

were drawn from a Gaussian distribution (mean $=$ 1 and variance $=$ 2). For the directed network the couplings were drawn from two Gaussian distributions with variance $=$ 2 and means equal to 1 and -2, respectively. In all cases, a significant fraction of both positive and negative couplings of different magnitudes are generated to test the reconstructions. There can be various types of dynamics that can approach the equilibrium Boltzmann distribution as long as the detailed balanced condition is satisfied. However, for general spin dynamical models, the system will not achieve equilibrium, and in some situations the system can reach a nonequilibrium steady-state (NESS) exhibiting a non-Boltzmann steady-state probability distribution, which is, in general, not easy to be characterized. The goal of the inverse Ising network problem is to infer J_{ij} from the time-series dynamics of the Ising spins $s_i(t)$, $i = 1, \ldots, N$, even if the underlying spin dynamical model is not known. In this paper, we shall consider the following different spin dynamics.

A. Glauber dynamics: Asynchronous update

The Ising-Glauber model [51] with asynchronous spin update is described by the probability of the spin i in the next time step to be $s_i(t+1)$ as

$$p[s_i(t+1)|s_i(t)] = \frac{1}{1+e^{-2\beta s_i(t+1)h_i(t)}};$$
$$h_i \equiv H_i(t) + \sum_j J_{ij} s_j(t), \qquad (7)$$

where $\beta \equiv 1/(k_B T)$, H_i is the local external field which can be time-dependent in general, and h_i represents the total field experienced by the spin i. Asynchronous dynamics refers to the situation that one spin selected randomly is updated in a MC step. For a symmetric $\mathbf{J}$ and time-independent external field, the dynamics will converge to the equilibrium state described by the Boltzmann distribution obeying a detailed balance and the fluctuation-dissipation theorem (FDT). In this

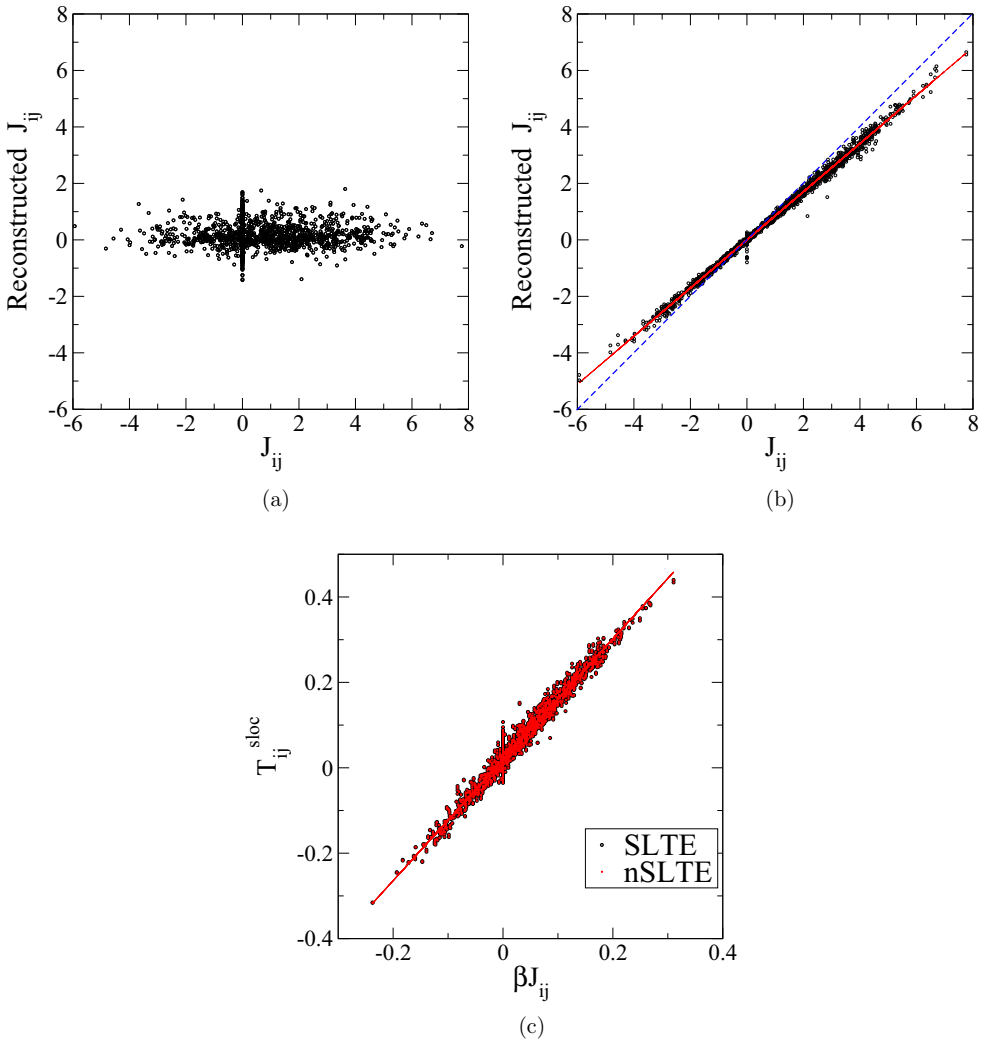

FIG. 3. Reconstruction of Ising spin couplings with synchronous update dynamics on a bidirectional weighted random network. J_{ij} are drawn from the same Gaussian distribution as in Fig. 1. Dynamics are generated by a 10^5 MCS/spin transient period for equilibration and then time-series of length 10^5 is used for coupling reconstruction. (a) Reconstructed J_{ij} vs. the actual ones using Eq. (8). (b) Reconstructed J_{ij} vs. the actual ones using Eq. (10). (c) T_{ij}^{sloc} (SLTE) and normalized T_{ij}^{sloc} (nSLTE) for every node pair ij vs. the actual coupling J_{ij}. The linear fits (solid lines) are also shown. The correlation coefficient between nSLTE and $J \simeq 0.96$.

case, the symmetric J_{ij} can be reconstructed by computing the equal-time spin correlation function via the FDT [14], one has

$$\mathbf{J} = \mathbf{D} - \mathbf{K}_0; \quad D_{ij} = \frac{\delta_{ij}}{1 - m_i^2}, \tag{8}$$

where $m_i \equiv \langle s_i \rangle$ is the average local magnetization of spin i, and the spin correlation functions are given by

$$(\mathbf{K}_\tau)_{ij} = \langle (s_i(t+\tau) - m_i)(s_j(t) - m_j) \rangle. \tag{9}$$

Figure 1 shows the pairwise TE and SLTE versus the actual coupling strengths for the asynchronous update Glauber dynamics with positive and negative couplings on a bidirectional random network computed from time-series after the system has achieved equilibrium. As shown in Fig. 1(a), the pairwise TE can be the same for positive and negative couplings and hence cannot distinguish the sign of the interactions. Furthermore, the variation of TE with the corresponding J_{ij} is nonlinear even one considers only the absolute values of the couplings. On the other hand, as shown in Fig. 1(b), both the SLTE and nSLTE obey a proportional relation with the corresponding actual values of J_{ij}, thus can faithfully reveal the signs and relative magnitudes of the couplings. It should be noted that such proportional relation is an empirical finding, so far it is found to hold for the Ising systems with various dynamical rules studied in the present study. Furthermore, the nSLTE also has a comparable magnitude with the dimensionless coupling βJ. In this equilibrium case, one can employ the FDT result in Eq. (8) to give a rather accurate reconstruction of J_{ij}, as shown in Fig. 1(c).

For the case of asymmetric $\mathbf{J}$ of the same link density ($p = 0.2$) [see Fig. 2(a)], the system is nonequilibrium even if there is no external field, but can achieve a steady-state which is non-Boltzmann. In this case, $\mathbf{J}$ can be reconstructed by computing the time-lag spin correlation functions from [17]

$$\mathbf{J} = \mathbf{D}\mathbf{K}_1\mathbf{K}_0^{-1}. \tag{10}$$

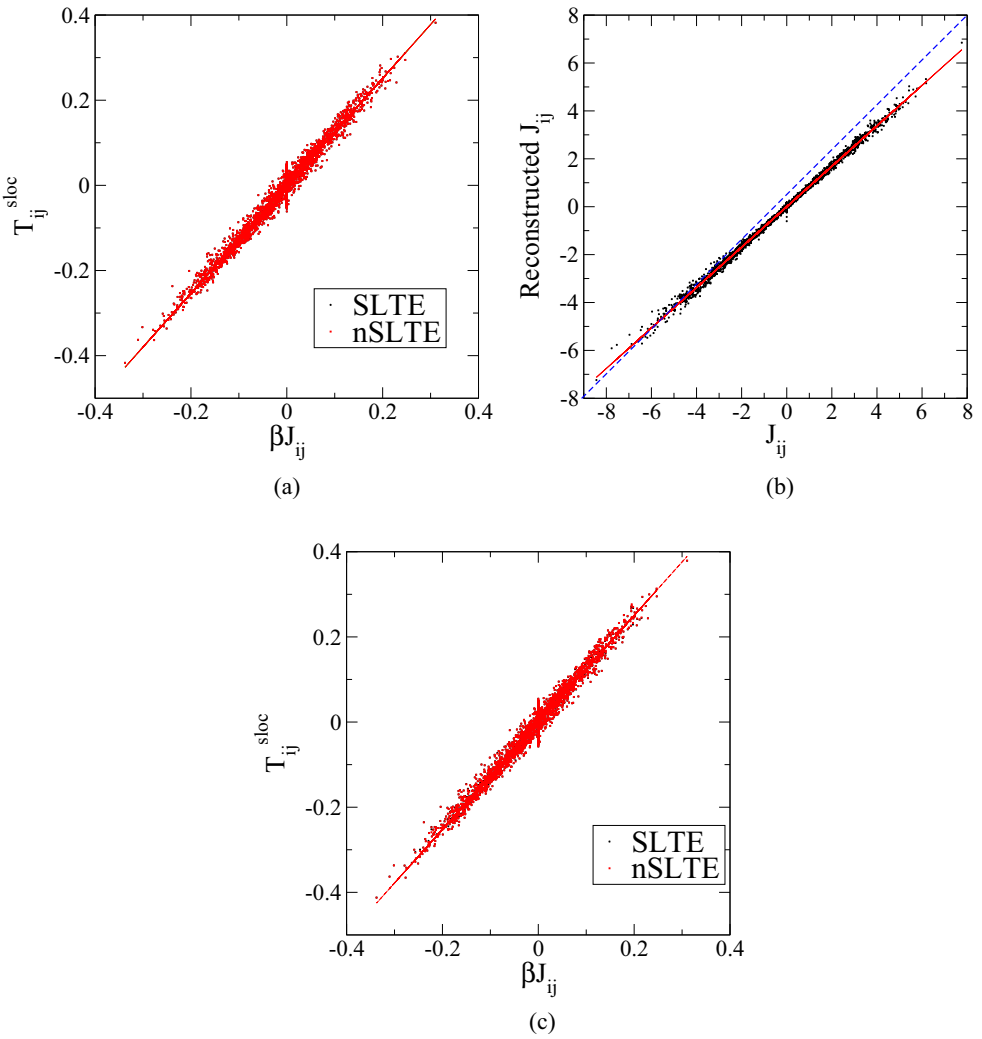

FIG. 4. Reconstruction of Ising spin couplings with synchronous update dynamics on a directed weighted random network. Dynamics are generated by a 10^5 MCS/spin transient period for equilibration and then time-series of length 10^5 is used for coupling reconstruction. (a) $T_{ij}^{\rm sloc}$ (SLTE) and normalized $T_{ij}^{\rm sloc}$ (nSLTE) for every node pair ij vs. the actual coupling J_{ij}, under no external field. The linear fits (solid lines) are also shown. The correlation coefficient between nSLTE and J $\simeq 0.96$. (b) Reconstructed J_{ij} vs. the actual ones using Eq. (10). The linear fitting (solid line) is also shown. (c) SLTE and nSLTE for every node pair ij vs. the actual coupling J_{ij}, in the presence of a nonuniform local external field. The linear fits (solid lines) are also shown. The correlation coefficient between nSLTE and J $\simeq 0.97$.

Figure 2 shows the pairwise TE and SLTE versus the actual coupling strengths for the case of asymmetric J_{ij} using time-series data after the system has reached the nonequilibrium steady state. Again the pairwise TE shows a quadratic variation with the actual coupling strengths whereas the SLTE and nSLTE show an approximate proportional relation with the J_{ij} covering the entire range of positive and negative couplings with a correlation coefficient $\sim$0.9. In addition, if one does not known *a priori* the dynamics of the system and naively using the FDT reconstruction formula (8) for equilibrium time-series, it will give poor reconstruction for the J_{ij}. One needs to use the proper reconstruction formula (10) to obtain satisfactory results, as shown in Fig. 2(d).

B. Glauber dynamics: Synchronous update

In contrast to the case of updating each spin independently and asynchronously, all the spins in the system are updated simultaneously in the synchronous-update Glauber dynamics according to the following probability:

$$p[\vec{s}(t+1)|\vec{s}(t)] = \prod_i \frac{1}{1+e^{-2\beta s_i(t+1)h_i(t)}}. \qquad (11)$$

In this case, regardless whether $\mathbf{J}$ is symmetric or not, the system will not satisfy a detailed balance but can reach a nonequilibrium steady state. For the case of symmetric J_{ij}, reconstruction results using time-series data after the system has reached the nonequilibrium steady state is shown in Fig. 3. Again the pairwise TE shows a quadratic variation with the actual coupling strengths (not shown) whereas the SLTE shows a proportional relation with the J_{ij} [Fig. 3(c)] with a correlation coefficient of $\sim$0.96. In this case, the reconstruction of $\mathbf{J}$ can be derived from naive mean-field theory and is given by Eq. (10) also [16]. Naively assuming equilibrium states and applying reconstruction formula (8)

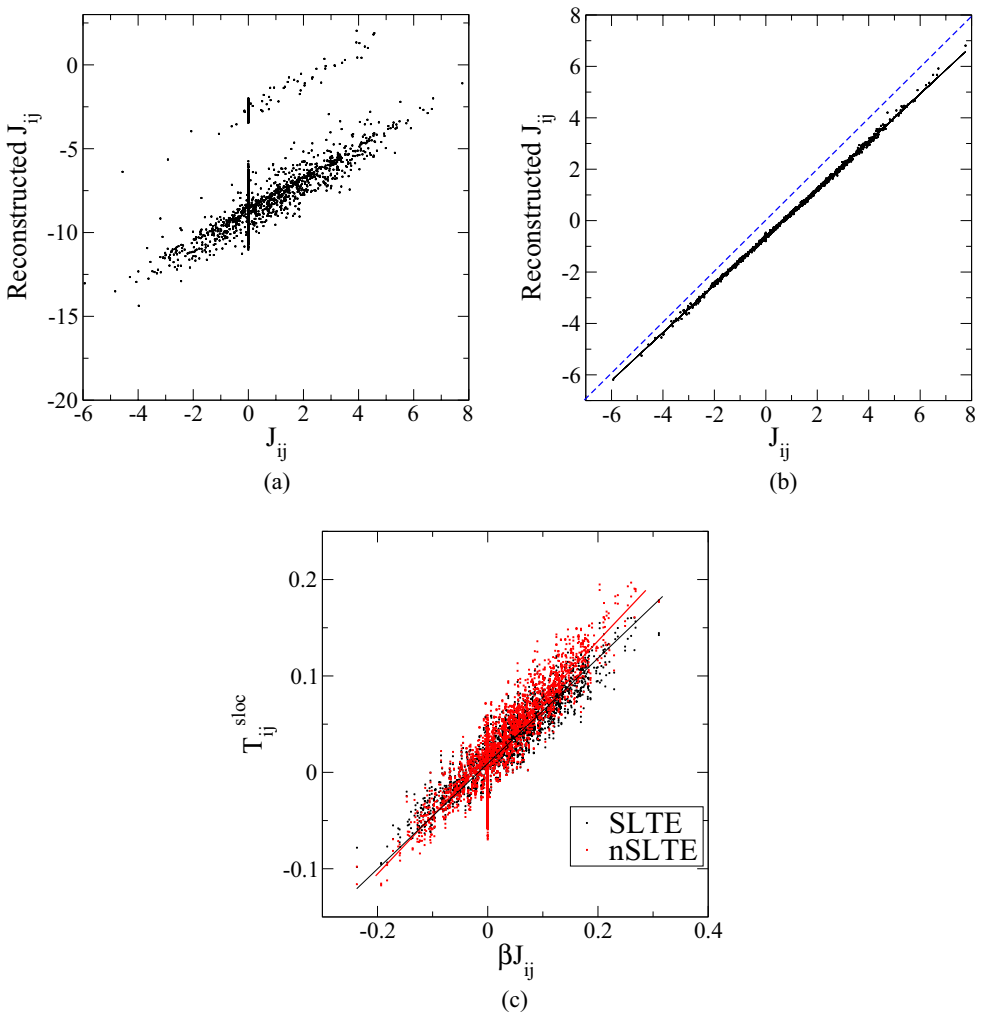

FIG. 5. Reconstruction of Ising spin couplings with Kawasaki dynamics on a bidirectional weighted random network. (a) Reconstructed J_{ij} vs. the actual ones using Eq. (8). Dynamics are generated by a 10^6 MCS/spin transient period for equilibration and then time-series of length 5×10^5 is used for coupling reconstruction. Panel (b) is similar to (a) with the same transient but followed by a time-series data four times the length as in (a) (2×10^6) for the system to achieve equilibrium. The linear fit (solid line) is also shown. (c) Computed SLTE using time-series data that has not fully achieved equilibrium. Dynamics are generated by a 10^5 MCS/spin transient period for equilibration and then followed by a time-series of length 2×10^5 is used for coupling reconstruction. The linear fits (solid lines) are also shown. The linear fits (solid lines) are also shown. The correlation coefficient between nSLTE and $J \simeq 0.83$.

will give poor results [see Fig. 3(a)], one needs to use the proper reconstruction formula (10) to reconstruct the coupling correctly [see Fig. 3(b)], again *a priori* knowledge of the dynamical model is essential. But using SLTE is model-free.

The case of asymmetric J_{ij} [with the same J_{ij} as in Fig. 2(a)] is also studied here. Figure 4(a) shows a proportional relation of SLTE with the couplings with a correlation coefficient of 0.97. The reconstruction using Eq. (10) is also shown in Fig. 4(b) for comparison. In addition, we also investigate the performance of SLTE for asynchronous update with asymmetric J_{ij} in the presence of a static nonuniform (zero-mean Gaussian distributed) local external field H_i. Again reconstruction using Eq. (8) gives poor result and one needs to use the proper reconstruction formula (10), which gives a performance similar to that of the case of no external field [Fig. 4(b)]. SLTE gives good reconstruction as displayed in Fig. 4(c) showing that SLTE again is proportional to the coupling strength.

C. Kawasaki spin exchange dynamics

In this case, the system obeys the global symmetry of conservation of total magnetization and spins are updated with the exchange of local interacting spin pairs. The probability of the spin pairs is given by

$$p[s_i(t+1), s_j(t+1)|s_i(t), s_j(t)] = \frac{1}{1+e^{-2\beta[s_i(t+1)(h_i(t)-h_j(t)]}}, \quad \text{for } s_i \neq s_j. \tag{12}$$

For symmetric **J**, the Kawasaki exchange dynamics obey the detailed balance condition and equilibrium Boltzmann distribution ill be achieved, but a non-equilibrium steady state will be reached for asymmetric **J**. However, the approach to the equilibrium or steady state is usually much slower due to the exchange dynamics. Here time is measured in Monte Carlo steps per spin (MCS/spin), one MCS/spin means that on

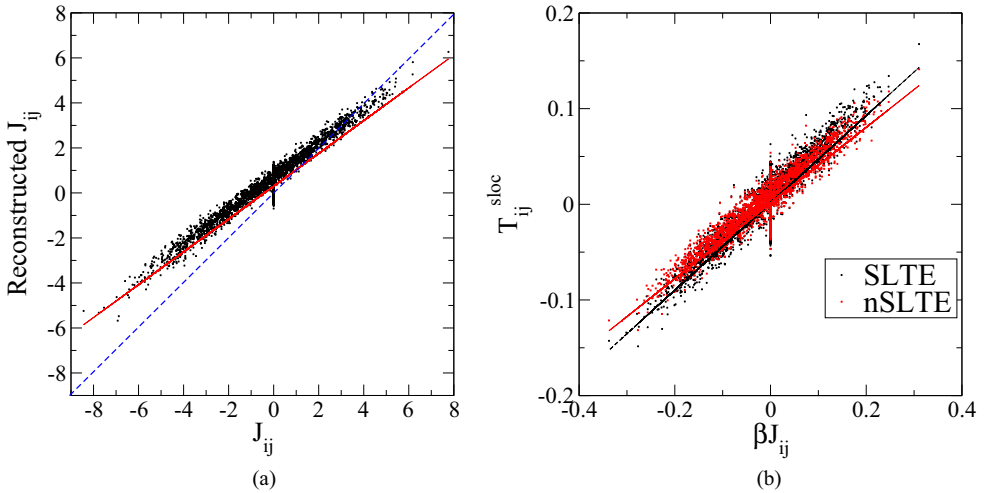

FIG. 6. Reconstruction of Ising spin couplings with Kawasaki dynamics on a directed weighted random network. Dynamics are generated by a 10^6 MCS/spin transient period for equilibration and followed by a time-series of length 2×10^6 is used for coupling reconstruction. (a) Reconstructed J_{ij} vs. the actual ones using Eq. (10). The linear fitting (solid line) is also shown. (b) T_{ij}^{sloc} (SLTE) and normalized T_{ij}^{sloc} (nSLTE) for every node pair ij vs. the actual coupling J_{ij}. The linear fittings (solid lines) are also shown. The correlation coefficient between nSLTE and J $\simeq 0.84$.

average each spin has attempted to update once. For symmetric **J**, with the *a priori* knowledge that the system can reach an equilibrium state, one can apply the FDT reconstruction formula for **J** in Eq. (8). After the system has equilibrated for some long (10^6 MCS/spin) time, spin time-series data are used for reconstruction using Eq. (8). But the reconstruction results are poor if an insufficient long time-series (5×10^5 MCS/spin) is used, as shown in Fig. 5(a) the reconstructed J_{ij} is bimodal with peaks at negative values which are way off from the known value of positive one. Very long time-series data are needed (2×10^6 MCS/spin) for satisfactory reconstruction, as shown in Fig. 5(b). This indicates that one needs to be sure that the system is well equilibrated to use the FDT reconstruction formula. On the other hand, the SLTE method can give relatively satisfactory reconstruction even when the time-series data used have not yet fully achieved equilibrium. Figure 5(c) shows the pairwise SLTE versus the actual coupling strengths for the case of symmetric J_{ij} using relatively short time-series data well before the system has equilibrated (10^5 MCS/spin transient followed by 2×10^5 time-series length for reconstruction). The proportionality of SLTE to the couplings is again satisfied. On the other hand, it should be noted that if the system is very far away from equilibrium and the time-series obtained for the system to approach to equilibrium is not sufficiently long, then SLTE cannot produce satisfactory reconstruction for the couplings. In the case if a long relaxation time-series is not available, but repeated independent shorter observations can be obtained, one could replace the time-average by ensemble average [52] to carry out the SLTE reconstruction.

For asymmetric **J**, the system is nonequilibrium but can achieve a steady state which is non-Boltzmann. In this case, **J** can be reconstructed by Eq. (10) to a less satisfactory level [see Fig. 6(a)] compared to the Glauber dynamics cases. On the other hand, the pairwise SLTE is well described by the proportionality to the J_{ij} as shown in Fig. 6(b).

IV. SUMMARY AND OUTLOOK

We demonstrated that the SLTE is an effective quantity to accurately reveal the pairwise couplings in the inverse Ising problem from time-series data of the spins, even when the underlying dynamical model is not known. The pairwise SLTE is well described by a proportionality relation to the corresponding coupling in the positive and negative domains, and thus making the extraction of the signs and relative coupling strengths reliable. In addition, the SLTE reconstruction performs well for equilibrium and nonequilibrium dynamical data, as illustrated in different kinetic Ising models. Two-state Ising dynamics are considered in this work; our method can be easily generalized to multistate discrete dynamics such as the Potts model. Furthermore, since TE calculations are also applicable to continuous variables, one expects SLTE can also be extended to such cases with an appropriate sorting kernel function. Taking into account the confounding effects in a network, we also anticipate that the sorting of conditional TE will further improve coupling strength reconstruction.

It should be noted that our method is not really changing the measure, but simply presenting a different summary of the local TE results that may be useful in circumstances aligning with excitatory or inhibitory couplings. Since no *a priori* knowledge for the details of the underlying dynamics is needed for the SLTE reconstruction, the method would have broad applications in various complex interacting systems. The general advantages of the SLTE method is (i) model-free and applicable in many different situations, (ii) works in situations where models do not or there is no known model, (iii) more data efficient in some situations. One direction in applications is to extract synaptic interactions in spiking neuronal data, not only one can obtain information about whether the synaptic connection is excitatory or inhibitory, one can infer also whether the neurons are excitatory or an inhibitory [43]. Real-time extraction of the nature and the strengths of the

synaptic coupling can help in designing feedback stimulation on the neuronal system for specific tasks or enhance learning schemes. Another application is on the gene-expression network time-series data to infer which gene is activating or suppressing the others in high throughput experiments.

ACKNOWLEDGMENT

This work has been supported by the Ministry of Science and Technology of Taiwan under Grant No. 107-2112-M-008-003-MY3, and NCTS of Taiwan.

[1] M. Timme, Europhys. Lett. **76**, 367 (2006).
[2] W. Wang, Y.-C. Lai, and C. Grebogi, Phys. Rep. **644**, 1 (2016).
[3] M. Nitzan, J. Casadiego, and M. Timme, Sci. Adv. **3**, e1600396 (2017).
[4] D. Yu, M. Righero, and L. Kocarev, Phys. Rev. Lett. **97**, 188701 (2006).
[5] M. Timme, Phys. Rev. Lett. **98**, 224101 (2007).
[6] S. G. Shandilya and M. Timme, New J. Phys. **13**, 013004 (2011).
[7] Z. Levnajić and A. Pikovsky, Phys. Rev. Lett. **107**, 034101 (2011).
[8] Z. Levnajić and A. Pikovsky, Sci. Rep. **4**, 5030 (2015).
[9] E. S. C. Ching, P.-Y. Lai, and C. Y. Leung, Phys. Rev. E **88**, 042817 (2013).
[10] E. S. C. Ching, P.-Y. Lai, and C. Y. Leung, Phys. Rev. E **91**, 030801(R) (2015).
[11] E. S. C. Ching and H. C. Tam, Phys. Rev. E **95**, 010301(R) (2017).
[12] P.-Y. Lai, Phys. Rev. E **95**, 022311 (2017).
[13] H. Tam, E. S. Ching, and P.-Y. Lai, Physica A (Amsterdam) **502**, 106 (2018).
[14] H. J. Kappen and F. B. Rodríguez, Neural Comput. **10**, 1137 (1998).
[15] Y. Roudi, J. Tyrcha, and J. Hertz, Phys. Rev. E **79**, 051915 (2009).
[16] Y. Roudi and J. A. Hertz, Phys. Rev. Lett. **106**, 048702 (2011).
[17] H.-L. Zeng, E. Aurell, M. Alava, and H. Mahmoudi, Phys. Rev. E **83**, 041135 (2011).
[18] H.-L. Zeng, M. Alava, E. Aurell, J. Hertz, and Y. Roudi, Phys. Rev. Lett. **110**, 210601 (2013).
[19] P. Zhang, J. Stat. Phys. **148**, 502 (2012).
[20] E. Aurell and M. Ekeberg, Phys. Rev. Lett. **108**, 090201 (2012).
[21] S. L. Dettmer, H. C. Nguyen, and J. Berg, Phys. Rev. E **94**, 052116 (2016).
[22] J. Albert and R. H. Swendsen, Phys. Proc. **57**, 99 (2014).
[23] J. Albert and R. H. Swendsen, Physica A (Amsterdam) **483**, 293 (2017).
[24] T. Schreiber, Phys. Rev. Lett. **85**, 461 (2000).
[25] T. Bossomaier, L. Barnett, M. Harré, and J. T. Lizier, *An Introduction to Transfer Entropy* (Springer International Publishing, Cham, Germany, 2016).
[26] L. Barnett, J. T. Lizier, M. Harré, A. K. Seth, and T. Bossomaier, Phys. Rev. Lett. **111**, 177203 (2013).
[27] F. Doria, R. Erichsen, Jr., D. Dominguez, M. González, and S. Magalhaes, Physica A (Amsterdam) **422**, 58 (2015).
[28] M. Li, Y. Fan, J. Wu, and Z. Di, Int. J. Mod. Phys. B **27**, 1350146 (2013).
[29] H. W. Lau and P. Grassberger, Phys. Rev. E **87**, 022128 (2013).
[30] Z. Deng, J. Wu, and W. Guo, Phys. Rev. E **90**, 063308 (2014).
[31] M. Wibral, R. Vicente, and J. T. Lizier, *Directed Information Measures in Neuroscience* (Springer, New York, 2014).
[32] S. Ito, M. E. Hansen, R. Heiland, A. Lumsdaine, A. M. Litke, and J. M. Beggs, PLoS ONE **6**, e27431 (2011).
[33] J. G. Orlandi, O. Stetter, J. Soriano, T. Geisel, D. Battaglia, and J. Garcia-Ojalvo, PLoS ONE **9**, e98842 (2014).
[34] H. P. Robinson, M. Kawahara, Y. Jimbo, K. Torimitsu, Y. Kuroda, and A. Kawana, J. Neurophysiol. **70**, 1606 (1993).
[35] L. C. Jia, M. Sano, P.-Y. Lai, and C. K. Chan, Phys. Rev. Lett. **93**, 088101 (2004).
[36] P.-Y. Lai, L. C. Jia, and C. K. Chan, Phys. Rev. E **73**, 051906 (2006).
[37] H. Song, C.-C. Chen, J.-J. Sun, P.-Y. Lai, and C. K. Chan, Phys. Rev. E **90**, 012703 (2014).
[38] M. Prokopenko, J. Lizier, and D. Price, Entropy **15**, 524 (2013).
[39] M. Prokopenko and I. Einav, Phys. Rev. E **91**, 062143 (2015).
[40] G. Ver Steeg and A. Galstyan, in *Proceedings of the 21st International Conference on World Wide Web* (ACM Press, New York, 2012), pp. 509–518.
[41] G. Ver Steeg and A. Galstyan, in *Proceedings of the Sixth ACM International Conference on Web Search and Data Mining* (ACM Press, New York, 2013), pp. 3–12.
[42] T. Tomokiyo and M. Hurst, in *Proceedings of the ACL 2003 Workshop on Multiword Expressions: Analysis, Acquisition and Treatment-Volume 18* (Association for Computational Linguistics, Stroudsburg, PA, 2003), pp. 33–40.
[43] F. Goetze, P.-Y. Lai, and C. Chan, BMC Neurosci. **16**, P30 (2015).
[44] J. T. Lizier, M. Prokopenko, and A. Y. Zomaya, Phys. Rev. E **77**, 026110 (2008).
[45] M. Pellicoro and S. Stramaglia, Physica A (Amsterdam) **389**, 4747 (2010).
[46] G. Bouma, in *Proceedings of the Biennial GSCL Conference* (Gunter Narr, Tübungen, Germany, 2009), Vol. 156, p. 31.
[47] C. Finn and J. T. Lizier, Entropy **20**, 826 (2018).
[48] B. Gourévitch and J. J. Eggermont, J. Neurophysiol. **97**, 2533 (2007).
[49] P. Erdős and A. Rényi, Publ. Math. Inst. Hung. Acad. Sci. **5**, 17 (1960).
[50] B. Bollobás, *Random Graphs* (Academic Press, London, 1985).
[51] R. J. Glauber, J. Math. Phys. **4**, 294 (1963).
[52] P. Wollstadt, M. Martínez-Zarzuela, R. Vicente, F. J. Díaz-Pernas, and M. Wibral, PLoS ONE **9**, e102833 (2014).